

Article

Urethane Synthesis in the Presence of Organic Acid Catalysts—A Computational Study

Hadeer Q. Waleed^{1,2}, Béla Viskolcz¹  and Béla Fiser^{1,3,4,*} ¹ Institute of Chemistry, University of Miskolc, 3515 Miskolc-Egyetemváros, Hungary² Higher Education and Industrial Cooperation Centre, University of Miskolc, 3515 Miskolc-Egyetemváros, Hungary³ Ferenc Rakoczi II Transcarpathian Hungarian College of Higher Education, 90200 Beregszász, Transcarpathia, Ukraine⁴ Department of Physical Chemistry, Faculty of Chemistry, University of Lodz, 90-236 Lodz, Poland

* Correspondence: bela.fiser@uni-miskolc.hu

Abstract: A general mechanism for catalytic urethane formation in the presence of acid catalysts, dimethyl hydrogen phosphate (DMHP), methanesulfonic acid (MSA), and trifluoromethanesulfonic acid (TFMSA), has been studied using theoretical methods. The reaction of phenyl isocyanate (PhNCO) and butan-1-ol (BuOH) has been selected to describe the energetic and structural features of the catalyst-free urethane formation. The catalytic activities of DMHP, MSA, and TFMSA have been compared by adding them to the PhNCO–BuOH model system. The thermodynamic properties of the reactions were computed by using the G3MP2BHandHLYP composite method. It was revealed that in the presence of trifluoromethanesulfonic acid, the activation energy was the lowest within the studied set of catalysts. The achieved results indicate that acids can be successfully employed in urethane synthesis and the mechanism was described.

Keywords: composite method; acid catalysts; polyurethane; polymers; materials



Citation: Waleed, H.Q.; Viskolcz, B.; Fiser, B. Urethane Synthesis in the Presence of Organic Acid Catalysts—A Computational Study. *Molecules* **2024**, *29*, 2375. <https://doi.org/10.3390/molecules29102375>

Academic Editor: Bryan M. Wong

Received: 18 April 2024

Revised: 11 May 2024

Accepted: 16 May 2024

Published: 17 May 2024



Copyright: © 2024 by the authors. Licensee MDPI, Basel, Switzerland. This article is an open access article distributed under the terms and conditions of the Creative Commons Attribution (CC BY) license (<https://creativecommons.org/licenses/by/4.0/>).

1. Introduction

The field of polymer science emerged to develop new materials for growing civil and military needs. It tends to be more interdisciplinary than most sciences, combining chemistry, chemical engineering, and other fields as well [1,2]. In 1937, one of the most special polymer types with versatile properties was discovered [3]. This special type of polymer is polyurethane (PU), which was developed by Otto Bayer to compete with nylon [4,5]. Bayer's invention ranks among the most important breakthroughs in polymer science. At the beginning of the 1950s, researchers were able to use PUs to produce soft foam plastic. In the early 1960s, synthetic PU adhesive, PU flexible fiber, and other types of PUs were developed [6]. From the mid-1960s to the 1990s, the development of polyurethanes significantly increased and they became unavoidable in many applications [7,8]. In 2018, the PU market reached USD 59.5 billion globally, and it is expected to grow between 2019 and 2026 by 5.8% CAGR (compound annual growth rate) [9,10]. Polyurethane is used in a large array of industries as flexible and rigid foams, elastomers, and thermoplastic materials [11]. Most of the PU types are designed to make life more comfortable and products more durable [12,13]. Polyurethanes (PUs) are a special group of heterochain polymers formed by the reaction of isocyanate (NCO) and hydroxyl (OH) groups [14,15]. Isocyanate is a chemical that contains at least one isocyanate group (-N=C=O) in its structure. In PU synthesis, two types of isocyanates, aromatic and aliphatic ones, are used [16]. The other main raw materials in PU synthesis are polyols containing two or more hydroxyl groups [17]. In addition to the effect of the chemical structure and the functionality of isocyanates and polyols on urethane formation [18], polyurethane synthesis can be finetuned by applying various additional compounds such as catalysts, chain extenders, crosslinkers, surfactants, and blowing agents [19]. In relation

to PU synthesis, catalysts are often used to accelerate the reaction rate of polynucleophiles with isocyanate groups or to promote the trimerization of the isocyanate group to form crosslinked polymers. In the production of PUs, the amount of applied catalysts is small, but their impact is significant [20]. Catalysts play an important role in the control and balance between the gelling and blowing reactions. They help to accurately control the relative reaction rates of the isocyanate with both alcohol and water. The imbalance between these reactions is one of the reasons for the collapse of foam or the formation of inappropriate cells that can be closed or opened prematurely [21,22]. Polyurethane catalysts mainly include organic acids, organic bases (amine catalysts), and organo-tin (organometallic) compounds [23–26]. Organic acid catalysts are a type of organic catalysts which show significant efficiency in urethane formation (alcohol–isocyanate) reactions [27]. The use of acid catalysis is expected to expand the range of metal-free polyurethane syntheses under both solution and bulk polymerization conditions [27]. Meanwhile, there are certain organic acids which are able to promote urethane formation under mild polymerization conditions and low catalyst loadings [28]. On the other hand, organic acid catalysts can extend the range of polymerizable monomers that have amides or additional functionalities that are sensitive to base catalysis [29]. The effect of organic acids on urethane formation has been investigated and the reaction between isocyanates and alcohols in the presence of these catalysts was studied at high temperatures. It was found that organic acids in certain aspects are more efficient in activating isocyanates than tin-based catalysts. Previously, the effect of amine catalysts on urethane formation using the phenyl isocyanate (PhNCO) -- butan-1-ol (BuOH) model reaction and the G3MP2BHandHLYP composite method was investigated. The accuracy of the method was validated by conducting kinetic experiments, and the theoretical results were in good agreement with the experimental ones. These results prove the validity of the proposed mechanism and verify the method selection as well [30–36]. Herein, the reaction between PhNCO and BuOH is studied in the presence of acid catalysts, dimethyl hydrogen phosphate (DMHP), methanesulfonic acid (MSA), and trifluoromethanesulfonic acid (TFMSA) (Figure 1). Dimethyl hydrogen phosphate is an organophosphorus compound. It is a colorless, odorless liquid that is miscible with water and many organic solvents. DMHP is versatile, making it valuable in various industrial and research settings with applications in chemical synthesis, catalysis, analytical chemistry, electrochemistry, and surfactant technology. Its ability to introduce phosphate groups into organic molecules makes it applicable in diverse areas [37,38], while methanesulfonic acid is a strong organic acid that is highly soluble in water and miscible with many organic solvents. This solubility makes it convenient for use in reactions. MSA is commonly used as a catalyst and acid promoter in organic synthesis reactions. It can facilitate a variety of reactions. Its strong acidity and compatibility with a wide range of substrates make it a versatile tool in synthetic chemistry [39,40]. Trifluoromethanesulfonic acid has several applications across various fields due to its strong acidity. TFMSA is widely used as a strong acid catalyst in various organic synthesis reactions. Its strong acidity promotes reaction rates and facilitates the formation of the desired products. TFMSA is utilized as a catalyst in different polymerization reactions, especially in the synthesis of polymers and copolymers. It can initiate polymerization reactions and control kinetics and molecular weight distributions [41,42]. Thus, these species can also be effective in urethane synthesis. To study the thermodynamic properties and understand the reactions from a mechanistic point of view, computational tools have been used.

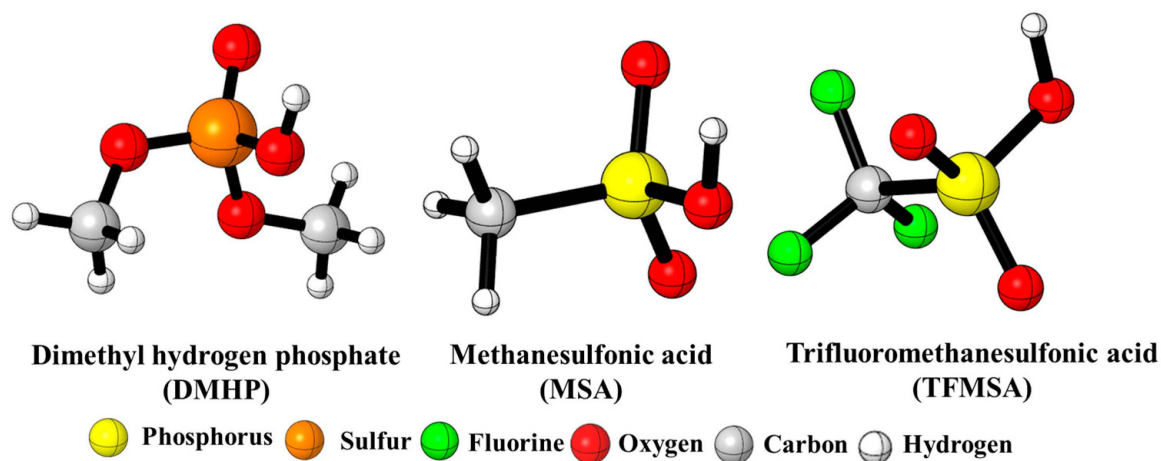


Figure 1. Three-dimensional structures of the studied catalysts.

2. Results and Discussion

The recently studied catalyst-free reaction mechanism was utilized as a reference [30,32–34] (Figure 2). The reaction between butan-1-ol (BuOH) and phenyl isocyanate (PhNCO) was selected as a model to describe the energetic and structural features of catalyst-free urethane formation. For the catalyst-free system, the corresponding thermodynamic properties were computed (Table 1).

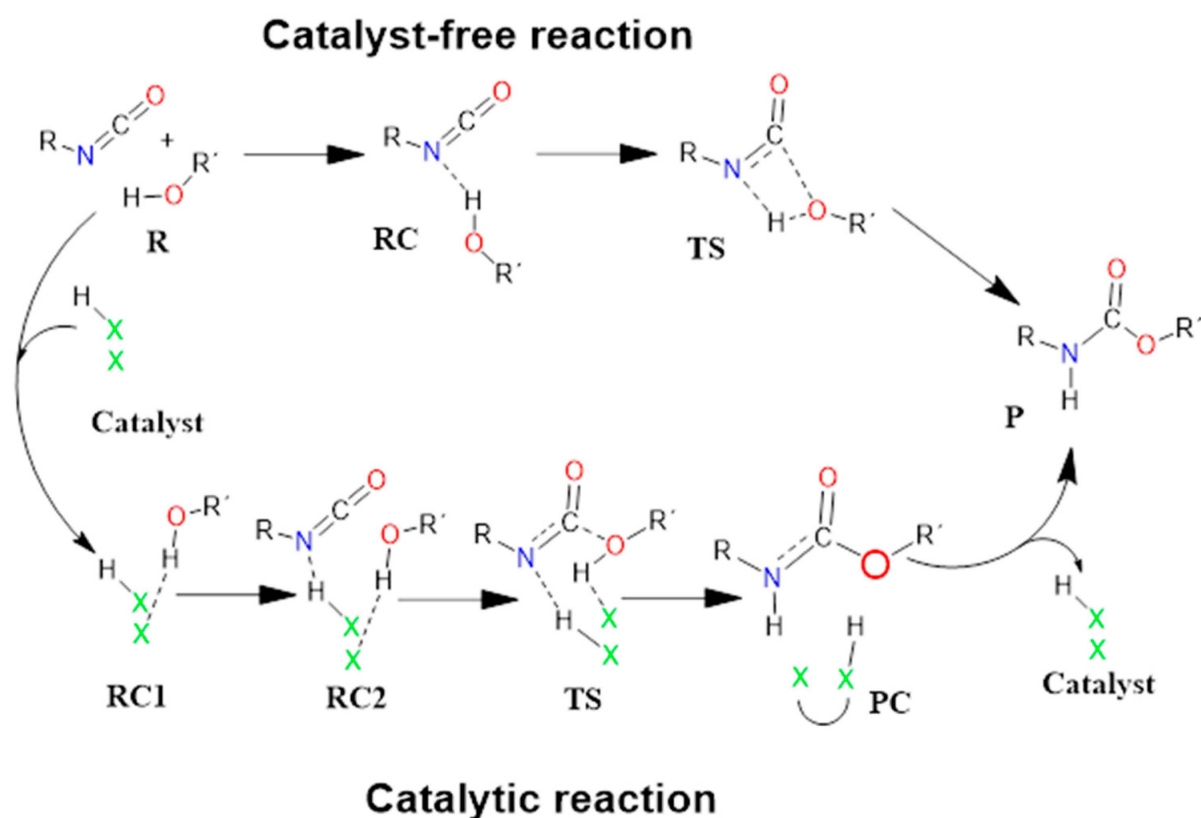


Figure 2. Schematic representation of the proposed general reaction mechanism of isocyanates and alcohols in the absence (upper row) and presence (bottom) of acid catalysts. RC—reactant complex; TS—transition state; PC—product complex; and P—product.

Table 1. The relative enthalpy ($\Delta_r H$) of the reaction between phenyl isocyanate and butan-1-ol with and without catalysts, calculated using the G3MP2BHandHLYP composite method (298.15 K and 1 atm) in acetonitrile, using the SMD implicit solvent model. R—reactant; RC—reactant complex; TS—transition state; PC—product complex; and P—product.

	$\Delta_r H$ (kJ/mol)					
	R	RC1	RC2	TS	PC	P
Catalyst-free system	0.00	-	-8.97 ^a	116.49	-	-94.84
DMHP	0.00	-18.09	-47.79	-15.31	-133.12	-94.84
MSA	0.00	-8.66	-41.30	-8.44	-125.01	-94.84
TFMSA	0.00	-6.94	-45.94	-42.85	-130.46	-94.84

^aRC for catalyst-free reaction.

From the optimized geometries (Figure 3), it can be observed that the urethane bond formed via a concerted mechanism.

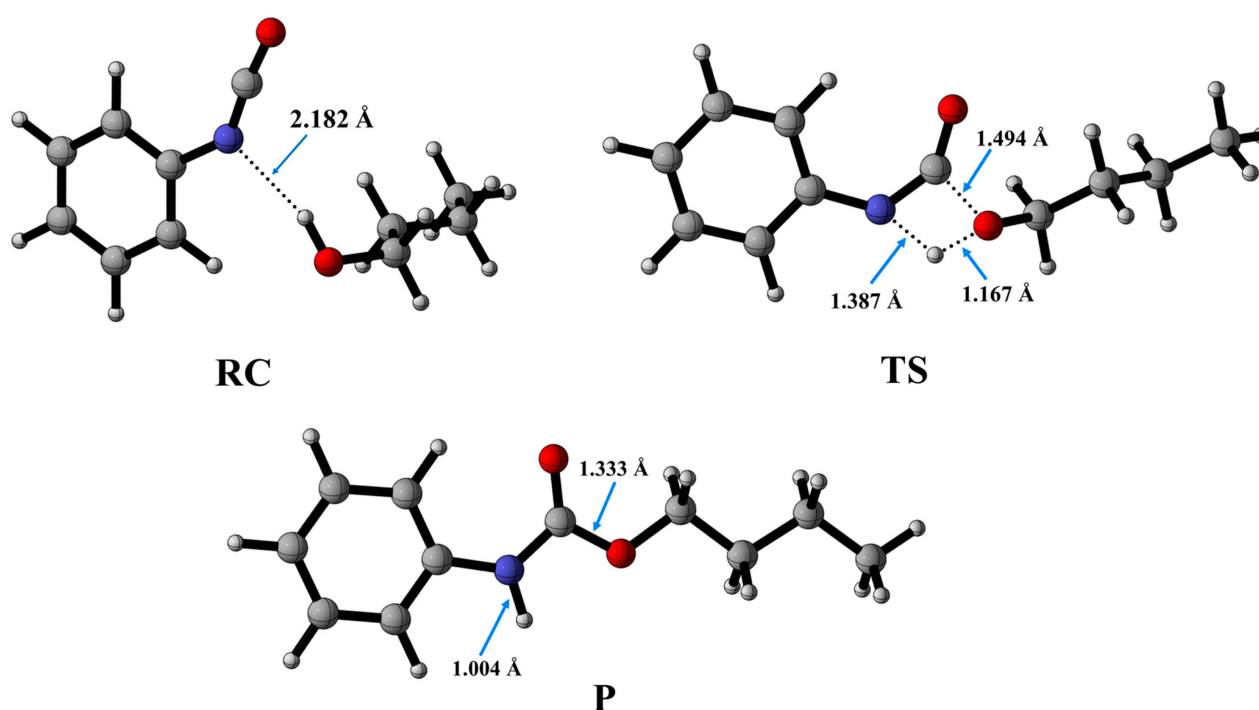


Figure 3. Optimized structures along the reaction pathway between phenyl isocyanate and butan-1-ol calculated at the BHandHLYP/6-31G(d) level of theory in acetonitrile at 298.15 K and 1 atm. RC—reactant complex; TS—transition state; P—product.

The process begins with the formation of the reactant complex (RC, PhNCO--BuOH) with a N-H distance of 2.182 Å, and the corresponding relative enthalpy is -8.97 (kJ/mol) (Figure 3). Following the reactant complex, a transition state (TS) is formed, within which a bond will form between the oxygen of the butan-1-ol and the carbon of the isocyanate group. The C-O distance in the TS is 1.494 Å. Additionally, hydrogen is donated from the butan-1-ol's hydroxyl group to the isocyanate's nitrogen, the N-H distance is decreased to 1.387 Å, and the relative enthalpy of the TS is 116.49 kJ/mol. Consequently, the final product (P) is achieved through the transition state, and the corresponding relative enthalpy is -94.84 kJ/mol (Figure 4).

In contrast to the catalyst-free case, urethane formation in the presence of acid catalysts includes five steps (Figure 2). First, a complex (RC1) between the alcohol and the catalyst forms, while the distance between the catalyst's oxygen and the hydroxyl hydrogen of

butan-1-ol is in the range of 1.830 and 2.048 Å (Figures 5–7) (Table 2, O-H*). This is supposed to mimic the industrial urethane synthesis, within which the catalyst is first mixed into the polyol. Then, in the next step, the isocyanate, in the current case PhNCO, is added to the system, and RC2, a trimolecular complex, is formed. In this step, a new interaction occurs between the butan-1-ol's oxygen and the isocyanate group, while only insignificant changes can be identified in the length of the previously established O-H*.

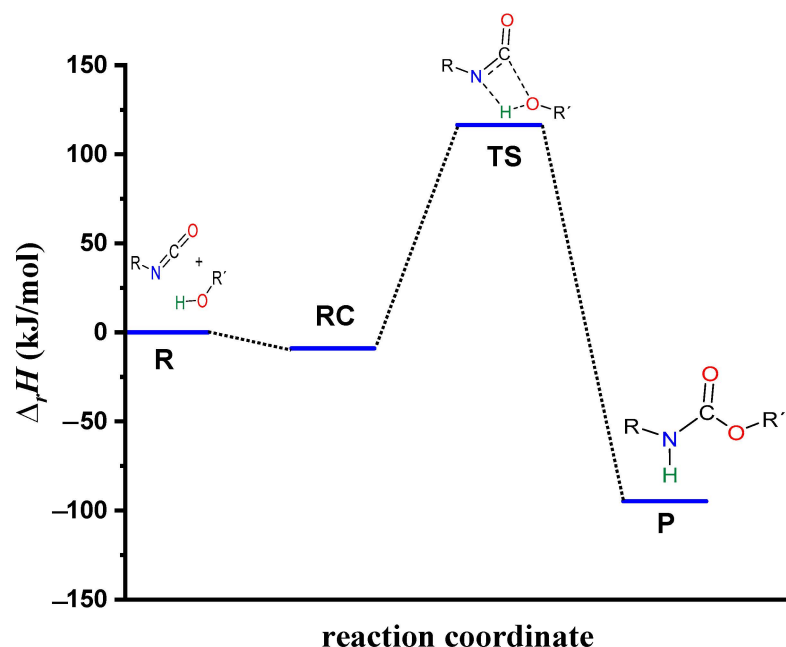


Figure 4. Energy profile (relative enthalpy ($\Delta_r H$)) of the catalyst-free phenyl isocyanate and butan-1-ol reaction calculated using the G3MP2BHandHLYP composite method in acetonitrile, using the SMD implicit solvent model at 298.15 K and 1 atm.

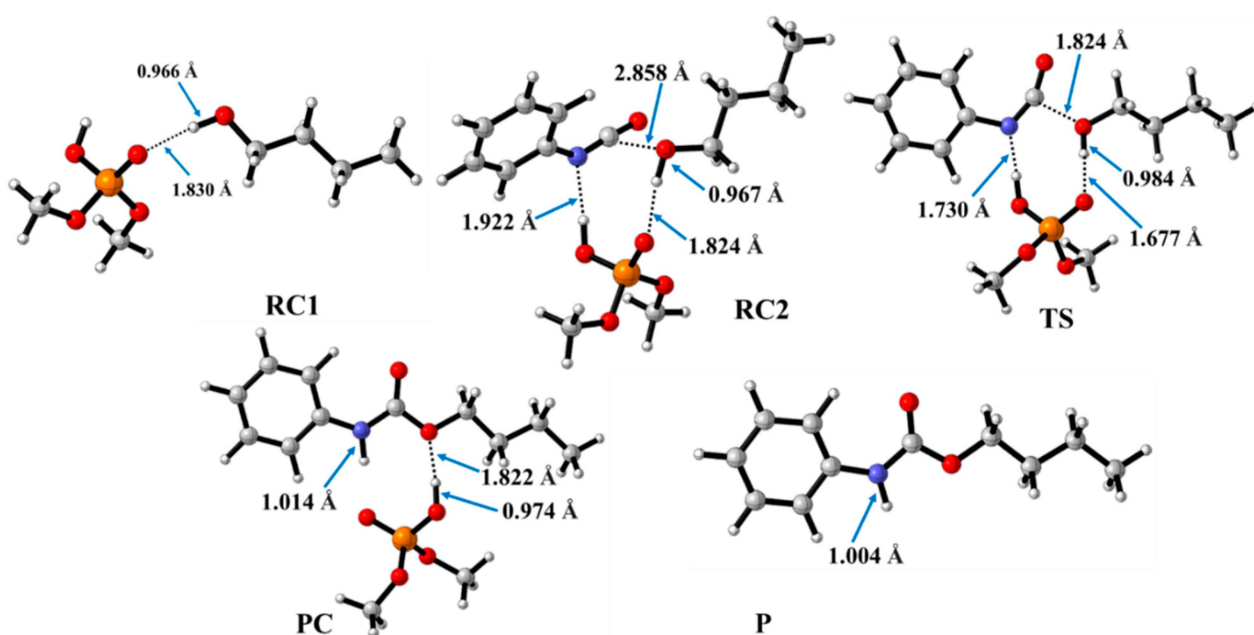


Figure 5. Optimized structures along the reaction pathway between phenyl isocyanate and butan-1-ol in the presence of dimethyl hydrogen phosphate (DMHP) calculated at the BHandHLYP/6-31G(d) level of theory (298.15 K and 1 atm) in acetonitrile. RC—reactant complex; TS—transition state; PC—product complex; and P—product.

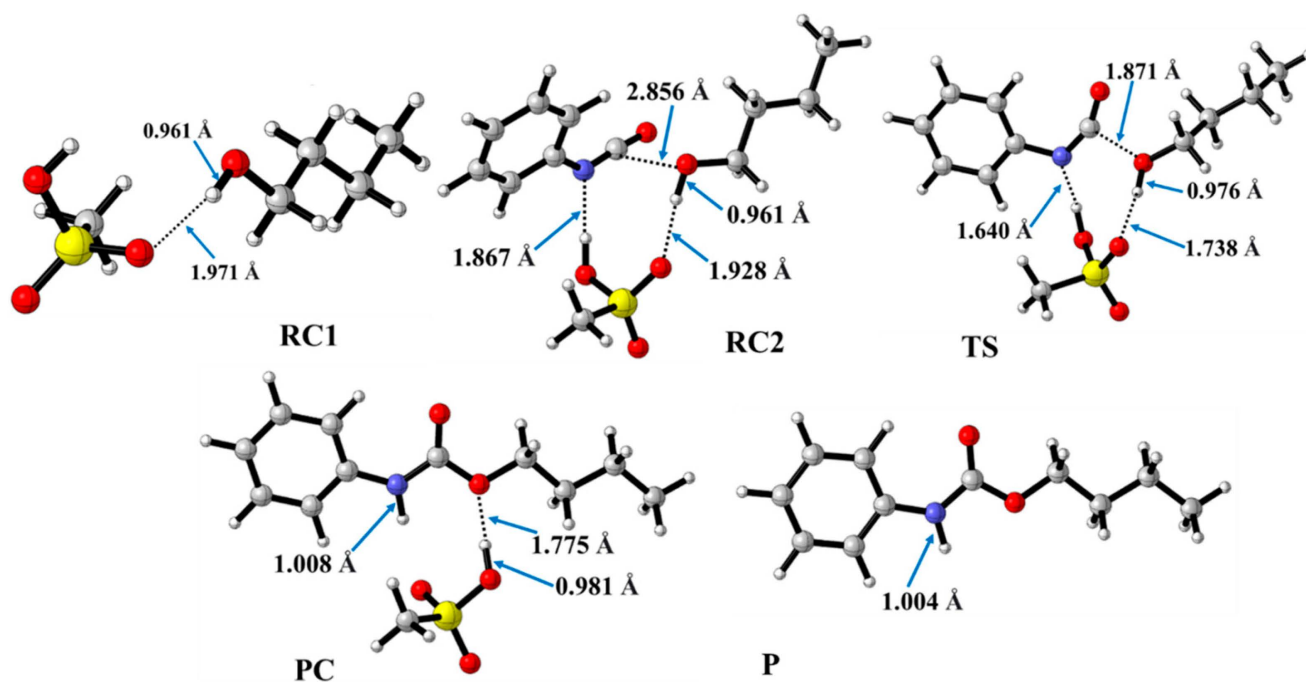


Figure 6. Optimized structures along the reaction pathway between phenyl isocyanate and butan-1-ol in the presence of methanesulfonic acid (MSA) calculated at the BHandHLYP/6-31G(d) level of theory (298.15 K and 1 atm) in acetonitrile. RC—reactant complex; TS—transition state; PC—product complex; and P—product.

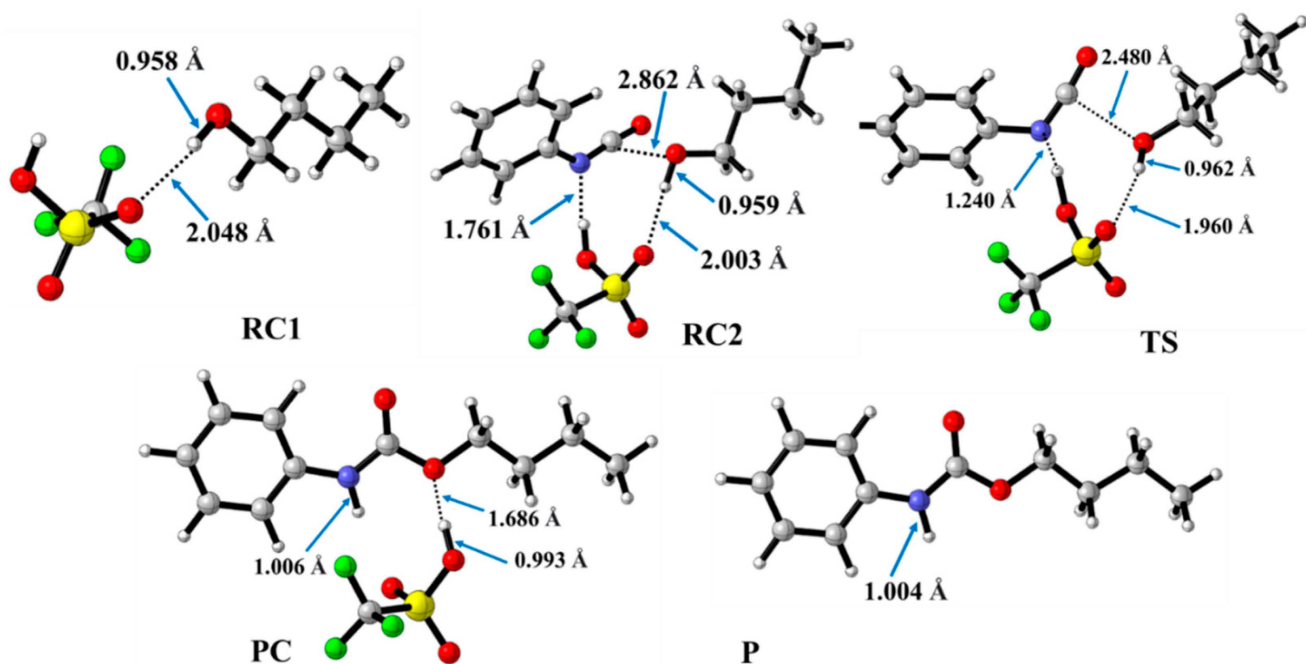


Figure 7. Optimized structures along the reaction pathway between phenyl isocyanate and butan-1-ol in the presence of trifluoromethanesulfonic acid (TFMSA) calculated at the BHandHLYP/6-31G(d) level of theory (298.15 K and 1 atm) in acetonitrile. RC—reactant complex; TS—transition state; PC—product complex; and P—product.

Table 2. N-H, O-H, and C-O bond lengths (Å) along the pathway of the phenyl isocyanate (PhNCO) and butan-1-ol reaction in the presence of the studied catalysts, dimethyl hydrogen phosphate (DMHP), methanesulfonic acid (MSA), and trifluoromethanesulfonic acid (TFMSA), calculated at the BHandHLYP/6-31G(d) level of theory (298.15 K and 1 atm) in acetonitrile. O-H* for catalysts; O-H** for butan-1-ol.

Catalysts	RC1		RC2				TS			PC		P		
	O-H*	O-H**	N-H	O-H*	O-H**	C-O	N-H	O-H*	O-H**	C-O	N-H	O-H*	O-H**	N-H
DMHP	1.830	0.966	1.922	1.824	0.967	2.858	1.730	1.677	0.984	1.824	1.014	0.974	1.822	1.004
MSA	1.971	0.961	1.867	1.928	0.961	2.856	1.640	1.738	0.967	1.871	1.008	0.981	1.775	1.004
TFMSA	2.048	0.958	1.761	2.003	0.959	2.862	1.240	1.960	0.962	2.480	1.006	0.993	1.686	1.004

The effect on the O-H** bond length is even smaller and almost no change is observed between RC1 and RC2 (Table 2). The most stable butan-1-ol–catalyst and trimolecular complexes are formed in the case of DMHP ($\Delta_r H = -18.09$ for RC1, and RC2, $\Delta_r H = -47.79$ kJ/mol). Meanwhile, the TFMSA–butan-1-ol complex is the least stable bimolecular complex ($\Delta_r H = -6.94$ kJ/mol), while the MSA–butan-1-ol–PhNCO complex is the least stable trimolecular complex (RC2, $\Delta_r H = -41.30$ kJ/mol) (Table 1 and Figure 8).

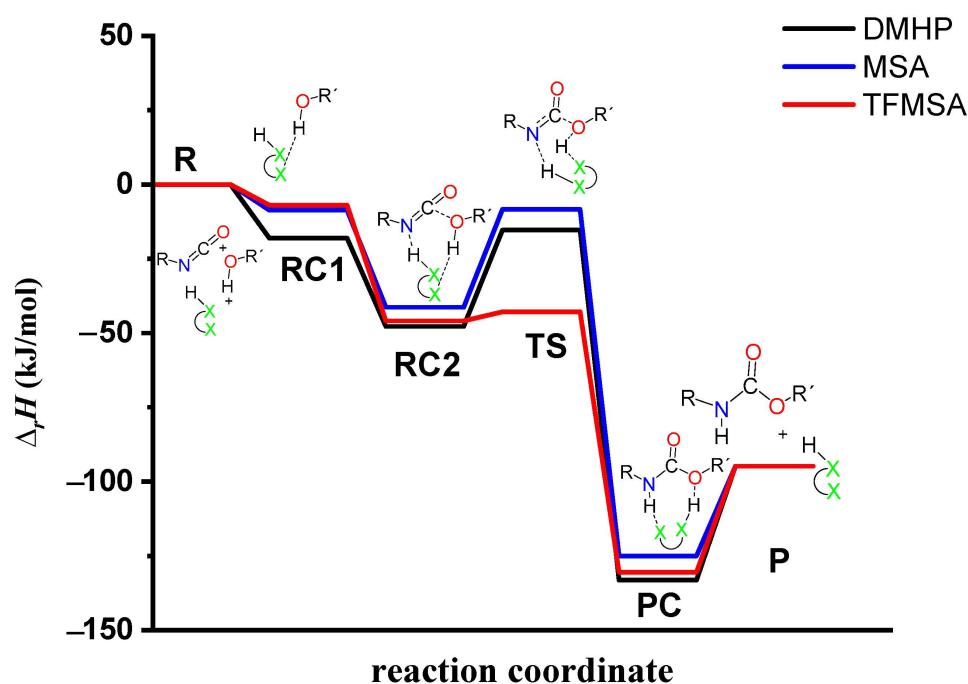


Figure 8. Relative enthalpy ($\Delta_r H$) profile of the studied catalyzed urethane formation reactions in the presence of dimethyl hydrogen phosphate (DMHP), methanesulfonic acid (MSA), and trifluoromethanesulfonic acid (TFMSA) calculated at the G3PMP2BHandHLYP level of theory (298.15 K and 1 atm) in acetonitrile using the SMD implicit solvent model, respectively.

In the next step, a transition state develops in the presence of the catalyst, where a proton transfer occurs from the hydroxyl group of butan-1-ol to the oxygen of the acid catalyst, resulting in a decrease in the O-H* distance, which ranges from 1.677 to 1.960 Å. Meanwhile, protons will be donated from the acid catalyst to the nitrogen of the isocyanate, with N-H distances ranging from 1.240 to 1.730 Å. Furthermore, a new bond will form between the carbon of the isocyanate group and the oxygen of butan-1-ol, significantly reducing the distances to 1.824–2.480 Å. At the same time, the O-H** distance increased. It was noticed that the C-O distance of TS is large for TFMSA compared to other catalysts. The variation in interatomic distances can be linked to the proton affinity, electronic structure,

and charge distribution of the acid. The potential energy curve shows that the relative enthalpy of the transition state is lowest (-42.85 kJ/mol) when trifluoromethanesulfonic acid is considered. In contrast, with dimethyl hydrogen phosphate and methanesulfonic acid, there are increases of ~ 27 kJ/mol and 51 kJ/mol, respectively (Figure 8). The results showed that the barrier height of the reaction in the presence of acid catalysts compared to the catalytic-free system ($\Delta\Delta_rH = \Delta_rH_{Cat.-free(RC-TS)} - \Delta_rH_{Cat.(RC1-TS)}$) significantly decreased by 127.7 , 125.3 , and 89.6 kJ/mol for DMHP, MSA, and TFMSA, respectively (Table 1, and Figure 8). It must be noted that the barrier height is computed as the enthalpy difference between the RC1 and TS, as the first step in the experiment is to mix the catalyst into the alcohol.

Before the reaction completes, a product complex (PC) forms where a bond is formed between the carbon of the isocyanate group and the oxygen of the butanol. Additionally, an N-H bond forms with distances ranging from 1.006 to 1.014 Å, and a PC relative enthalpy range of -125.01 and -133.12 kJ/mol. At this point, the catalyst is released, and the urethane bond is already complete (Figures 5–7). In the final step, the catalysts and the product are separated (P), with the corresponding relative enthalpy of -94.84 kJ/mol where both the strength of a given acid and the nucleophilicity of its conjugate base play a vital role in the bifunctional catalysis of urethane formation. Therefore, along with the whole reaction mechanism, the trifluoromethanesulfonic acid (TFMSA) catalyst was the most effective and provided the most favorable pathway.

3. Methods

The molecules were optimized by using the BHandHLYP (Becke, Half-and-Half, Lee–Yang–Parr) [43] density functional method in combination with the 6-31G(d) [44–46] basis set. The effect of the solvent (e.g., acetonitrile, MeCN, $\epsilon_r = 35.688$) was also considered by employing the SMD polarizable continuum model [47]. Several different density functional theory methods such as B3LYP [48], BHandHLYP [43], and ω B97X-D [49], in combination with the 6-31G(d) [44–46] basis set, were tested to investigate urethane formation using organic catalysts. However, only the BHandHLYP method was able to identify all the critical points on the potential energy surfaces (PESs) of the studied catalytic processes, proving its efficiency in studying catalytic urethane formation reactions [30,34,35,50]. Furthermore, to determine the thermodynamic properties of the studied system and to verify the nature of the stationary points on the potential energy surface, frequency calculations were performed. Meanwhile, to further improve the accuracy of the results, the G3MP2BHandHLYP composite method [50–52] was applied. On each optimized structures, two separate single-point energy calculations were performed at the QCISD(T)/6-31G(d) and MP2/GTMP2Large levels of theory and the previously determined composite scheme was applied [53,54].

All the calculations were carried out using the Gaussian 09 program [55]. The geometric configurations in this study were all displayed by using the CYLview program [56].

4. Conclusions

Urethane formation in organic acid-catalyzed processes was studied using computational chemical tools, including both density functional theory (BHandHLYP/6-31G(d)) and composite methods (G3MP2BHandHLYP). A general mechanism for catalytic urethane formation in the presence of three different acid catalysts, dimethyl hydrogen phosphate (DMHP), methanesulfonic acid (MSA), and trifluoromethanesulfonic acid (TFMSA), has been examined and described. The reaction mechanism of acid-catalyzed urethane formation contains five steps, which include one transition state and product complex. This route is different from the mechanism for catalytic urethane formation in the presence of amine catalysts. Meanwhile, it is slightly similar to the catalyst-free process as both have one transition state. However, the results showed that the barrier height of the reaction in the presence of acid catalysts compared to the catalyst-free system ($\Delta\Delta_rH = \Delta_rH_{Cat.-free(RC-TS)} - \Delta_rH_{Cat.(RC1-TS)}$) significantly decreased by 127.7 , 125.3 , and 89.6 kJ/mol for DMHP, MSA, and TFMSA, respectively. It was found that TFMSA was the

most potent organic acid catalyst within the studied set of species. This finding can be used to design better candidates for future synthetic explorations.

Supplementary Materials: The following supporting information can be downloaded at: <https://www.mdpi.com/article/10.3390/molecules29102375/s1>, Tables S1 and S2: Thermodynamic properties calculated at the BHandHLYP/6-31G(d) and G3MP2BHandHLYP levels of theory. Table S3: Cartesian coordinates of the stationary points for the studied species.

Author Contributions: The manuscript was written through the contributions of all authors. H.Q.W., B.F. and B.V. developed the original concept of the paper. H.Q.W. and B.F. wrote the paper. H.Q.W. carried out the calculations. Formal analysis of the results was carried out by H.Q.W. and B.V. and B.F., B.V. and B.F. contributed equally to scoping and structuring the paper and provided additional guidance on computational methods. All authors have read and agreed to the published version of the manuscript.

Funding: This research was supported by the National Research, Development and Innovation Fund (Hungary) within the TKP2021-NVA-14 project. H.Q.W. received support from the ÚNKP-23-3-II. New National Excellence Program of the Ministry for Culture and Innovation from the source of the National Research, Development, and Innovation Fund. This research was funded in part by the National Science Centre, Poland under the MINIATURA 7 call within the project reg. No: 2023/07/X/ST4/01433.

Institutional Review Board Statement: Not applicable.

Informed Consent Statement: Not applicable.

Data Availability Statement: The structures, figures, and additional tables are available in the Supplementary Materials.

Acknowledgments: The GITDA (Governmental Information-Technology Development Agency, Hungary) is gratefully acknowledged for allocating the computing resources used in this work. Further calculations were carried out using resources provided by the Wroclaw Centre for Networking and Supercomputing.

Conflicts of Interest: The authors declare no conflicts of interest.

References

1. Kanamori, T.; Sakai, K. Introduction to Polymer Science Involved in Membrane Preparation Technology. *Nihon Rinsho Jpn. J. Clin. Med.* **1991**, *49*, 44–52.
2. Saldívar-Guerra, E.; Vivaldo-Lima, E. *Handbook of Polymer Synthesis, Characterization, and Processing*; Wiley: Hoboken, NJ, USA, 2013; pp. 1–622. [[CrossRef](#)]
3. Szycher, M. Structure–property relations in polyurethanes. In *Szycher's Handbook of Polyurethanes*, 2nd ed.; CRC Press: Boca Raton, FL, USA, 2012; ISBN 9781439863138.
4. Yanping, Y. The Development of Polyurethane. *Mater. Sci. Mater. Rev.* **2018**, *1*, 1–8. [[CrossRef](#)]
5. Bayer, O. Das Di-Isocyanat-Polyadditionsverfahren (Polyurethane). *Angew. Chem.* **1947**, *59*, 257–288. [[CrossRef](#)]
6. Das, A.; Mahanwar, P. A Brief Discussion on Advances in Polyurethane Applications. *Adv. Ind. Eng. Polym. Res.* **2020**, *3*, 93–101. [[CrossRef](#)]
7. Brzeska, J.; Piotrowska-Kirschling, A. A Brief Introduction to the Polyurethanes According to the Principles of Green Chemistry. *Processes* **2021**, *9*, 1929. [[CrossRef](#)]
8. Matsumura, S.; Soeda, Y.; Toshima, K. Perspectives for Synthesis and Production of Polyurethanes and Related Polymers by Enzymes Directed toward Green and Sustainable Chemistry. *Appl. Microbiol. Biotechnol.* **2006**, *70*, 12–20. [[CrossRef](#)]
9. Polyurethanes Market Statistics, PU Share 2026 PDF Report. Available online: <https://www.gminsights.com/industry-analysis/polyurethane-PU-market-report> (accessed on 8 September 2021).
10. Polyurethane Foam Market: Trends, Opportunities and Competitive Analysis. Available online: <https://www.lucintel.com/polyurethane-foam-market.aspx> (accessed on 11 July 2022).
11. Sabrina, S.S.A.; Denilson, A.S.; Danielle, M.A. Physico-Chemical Analysis of Flexible Polyurethane Foams Containing Commercial Calcium Carbonate. *Mater. Res.* **2008**, *11*, 433–438. [[CrossRef](#)]
12. Sonnenschein, M.F. *Polyurethanes: Science, Technology, Markets, and Trends*; John Wiley & Sons, Inc.: Hoboken, NJ, USA, 2015; ISBN 978-1-118-73783-5.
13. Suleman, S.; Khan, S.M.; Gull, N.; Aleem, W.; Shafiq, M.; Jamil, T. Comprehensive Short Review on Polyurethane Foam. *Int. J. Innov. Appl. Stud.* **2014**, *12*, 165–169.

14. Ionescu, M. *Chemistry and Technology of Polyols for Polyurethanes*, 2nd ed.; A Smithers Group Company Shawbury: Shrewsbury, UK, 2016; Volume 1, ISBN 9781910242988.
15. Zhang, X.D.; Neff, R.A.; Macosko, C.W. Foam Stability in Flexible Polyurethane Foam Systems. In *Polymeric Foams: Mechanisms and Materials*; CRC Press: Boca Raton, FL, USA, 2004; pp. 139–172, ISBN 9780203506141.
16. Aqilahhamuzan, H.; Badri, K.H. The Role of Isocyanates in Determining the Viscoelastic Properties of Polyurethane. In *AIP Conference Proceedings*; AIP Publishing: College Park, MD, USA, 2016; Volume 1784. [[CrossRef](#)]
17. Radeloff, M.A.; Beck, R.H.F. Polyols—More than Sweeteners. *Sugar Ind.* **2013**, *226*–234. [[CrossRef](#)]
18. Echeverria-Altuna, O.; Ollo, O.; Calvo-Correas, T.; Harismendy, I.; Eceiza, A. Effect of the Catalyst System on the Reactivity of a Polyurethane Resin System for RTM Manufacturing of Structural Composites. *Express Polym. Lett.* **2022**, *16*, 234–247. [[CrossRef](#)]
19. Touchet, T.J.; Cosgriff-Hernandez, E.M. *Hierarchical Structure-Property Relationships of Segmented Polyurethanes*; Elsevier Ltd.: Amsterdam, The Netherlands, 2016; ISBN 9780081006221.
20. Gao, Z.; Wang, Z.; Liu, Z.; Fu, L.; Li, X.; Eling, B.; Pösel, E.; Schander, E.; Wang, Z. Hard Block Length Distribution of Thermoplastic Polyurethane Determined by Polymerization-Induced Phase Separation. *Polymer* **2022**, *256*, 125236. [[CrossRef](#)]
21. De Souza, F.M.; Kahol, P.K.; Gupta, R.K. Introduction to Polyurethane Chemistry. In *Polyurethane Chemistry: Renewable Polyols and Isocyanates*; American Chemical Society: Washington, DC, USA, 2021; Volume 1380, pp. 1–24. [[CrossRef](#)]
22. Rao, R.R.; Mondy, L.A.; Long, K.N.; Celina, M.C.; Wyatt, N.; Roberts, C.C.; Soehnel, M.M.; Brunini, V.E. The Kinetics of Polyurethane Structural Foam Formation: Foaming and Polymerization. *AIChE J.* **2012**, *59*, 215–228.
23. Ruiduan, L.; Ling, L.; Yanjie, L.; Ben, W.; Jun, Y.J.; Jibo, Z. Research Progress of Amine Catalysts for Polyurethane. *New Mater. Intell. Manuf.(NMIM)* **2018**, *1*, 54–57. [[CrossRef](#)]
24. Sardon, H.; Chan, J.M.; Ono, R.J.; Mecerreyes, D.; Hedrick, J.L. Highly Tunable Polyurethanes: Organocatalyzed Polyaddition and Subsequent Post-Polymerization Modification of Pentafluorophenyl Ester Sidechains. *Polym. Chem.* **2014**, *5*, 3547–3550. [[CrossRef](#)]
25. Malwitz, N.; Wong, S.W.; Frisch, K.C.; Manis, P.A. Amine Catalysis of Polyurethane Foams. *J. Cell. Plast.* **1987**, *23*, 461–502. [[CrossRef](#)]
26. Rad, A.S.; Ardjmand, M. Studying on the Mechanism and Raw Materials Used to Manufacturing Polyurethane. *Transportation* **2008**, *3*, 60–71.
27. Sardon, H.; Engler, A.C.; Chan, J.M.; Garcia, J.M.; Coady, D.J.; Pascual, A.; Mecerreyes, D.; Jones, G.O.; Rice, J.E.; Horn, H.W.; et al. Organic Acid-Catalyzed Polyurethane Formation via a Dual-Activated Mechanism: Unexpected Preference of n-Activation over o-Activation of Isocyanates. *J. Am. Chem. Soc.* **2013**, *135*, 16235–16241. [[CrossRef](#)] [[PubMed](#)]
28. Chen, Z.J.; Zhong, W.Q.; Tang, D.L.; Zhang, G.Z. Preparation of Organic Nanoacid Catalyst for Urethane Formation. *Chin. J. Chem. Phys.* **2017**, *30*, 339–342. [[CrossRef](#)]
29. Dove, A.P. Organic Catalysis for Ring-Opening Polymerization. *ACS Macro Lett.* **2012**, *1*, 1409–1412. [[CrossRef](#)]
30. Waleed, H.Q.; Csécsi, M.; Konyhás, V.; Boros, Z.R.; Viskolcz, B.; Fejes, Z.; Fiser, B. Aliphatic Tertiary Amine Catalysed Urethane Formation—A Combined Experimental and Theoretical Study. *Phys. Chem. Chem. Phys.* **2022**, *24*, 20538. [[CrossRef](#)]
31. Waleed, H.Q.; Hadjadj, R.; Viskolcz, B.; Fiser, B. Stoichiometric Reaction and Catalytic Effect of 2-Dimethylaminoethanol in Urethane Formation. *Phys. Chem. Chem. Phys.* **2024**, *26*, 7103–7108. [[CrossRef](#)] [[PubMed](#)]
32. Waleed, H.Q.; Viskolcz, B.; Fejes, Z.; Fiser, B. Urethane Formation in the Presence of 2,2-Dimorpholinodiethylether (DMDEE) and 1,4-Dimethylpiperazine (DMP)—A Combined Experimental and Theoretical Study. *Comput. Theor. Chem.* **2023**, *1221*, 114045. [[CrossRef](#)]
33. Waleed, H.Q.; Hadjadj, R.; Viskolcz, B.; Fiser, B. Effect of Morpholine, and 4-Methylmorpholine on Urethane Formation: A Computational Study. *Sci. Rep.* **2023**, *13*, 17950. [[CrossRef](#)] [[PubMed](#)]
34. Waleed, H.Q.; Pecsmány, D.; Csécsi, M.; Farkas, L.; Viskolcz, B.; Fejes, Z.; Fiser, B. Experimental and Theoretical Study of Cyclic Amine Catalysed Urethane Formation. *Polymers* **2022**, *14*, 2859. [[CrossRef](#)] [[PubMed](#)]
35. Waleed, H.Q.; Csécsi, M.; Hadjadj, R.; Thangaraj, R.; Pecsmány, D.; Owen, M.; Szőri, M.; Fejes, Z.; Viskolcz, B.; Fiser, B. Computational Study of Catalytic Urethane Formation. *Polymers* **2022**, *14*, 8. [[CrossRef](#)] [[PubMed](#)]
36. Waleed, H.Q.; Csécsi, M.; Hadjadj, R.; Thangaraj, R.; Pecsmány, D.; Owen, M.; Szőri, M.; Fejes, Z.; Viskolcz, B.; Fiser, B. The Catalytic Effect of DBU on Urethane Formation—A Computational Study. *Mater. Sci. Eng.* **2021**, *46*, 70–77.
37. IARC. Dimethyl Hydrogen Phosphite. In *Monographs on the Evaluation of Carcinogenic Risk of Chemicals to Humans*; IARC: Lyon, France, 1990; Volume 71, pp. 1437–1440.
38. Nomeir, A.A.; Burka, L.T.; Matthews, H.B. Analysis of Dimethyl Hydrogen Phosphite and Its Stability under Simulated Physiological Conditions. *J. Anal. Toxicol.* **1988**, *12*, 334–338. [[CrossRef](#)] [[PubMed](#)]
39. Roitman, D.B.; McAlister, J.; Oaks, F.L. Composition Characterization of Methanesulfonic Acid. *J. Chem. Eng. Data* **1994**, *39*, 56–60. [[CrossRef](#)]
40. Methanesulfonic Acid. *Safety Data Sheet*; No. 1907/2006 (REACH); Chemos GmbH&Co.KG: Altdorf, Germany, 2019.
41. Kazakova, A.N.; Vasilyev, A.V. Trifluoromethanesulfonic Acid in Organic Synthesis. *Russ. J. Org. Chem.* **2017**, *53*, 485–509. [[CrossRef](#)]
42. Marziano, N.C.; Ronchin, L.; Tortato, C.; Zingales, A.; Sheikh-Osman, A.A. Acidity and Reactivity of Trifluoromethanesulfonic Acid in Liquid and Solid Acid Catalysts. *J. Mol. Catal. A Chem.* **2001**, *174*, 265–277. [[CrossRef](#)]
43. Becke, A.D. A New Mixing of Hartree-Fock and Local Density-Functional Theories. *J. Chem. Phys.* **1993**, *98*, 1372–1377. [[CrossRef](#)]

44. Ditchfield, R.; Hehre, W.J.; Pople, J.A. Self-Consistent Molecular-Orbital Methods. IX. An Extended Gaussian-Type Basis for Molecular-Orbital Studies of Organic Molecules. *J. Chem. Phys.* **1971**, *54*, 720–723. [[CrossRef](#)]
45. Rassolov, V.A.; Pople, J.A.; Ratner, M.A.; Windus, T.L. 6-31G* Basis Set for Atoms K through Zn. *J. Chem. Phys.* **1998**, *109*, 1223–1229. [[CrossRef](#)]
46. Petersson, G.A.; Bennett, A.; Tensfeldt, T.G.; Al-Laham, M.A.; Shirley, W.A.; Mantzaris, J. A Complete Basis Set Model Chemistry. I. The Total Energies of Closed-Shell Atoms and Hydrides of the First-Row Elements. *J. Chem. Phys.* **1988**, *89*, 2193–2218. [[CrossRef](#)]
47. Marenich, A.V.; Cramer, C.J.; Truhlar, D.G. Universal Solvation Model Based on Solute Electron Density and on a Continuum Model of the Solvent Defined by the Bulk Dielectric Constant and Atomic Surface Tensions. *J. Phys. Chem. B* **2009**, *113*, 6378–6396. [[CrossRef](#)]
48. Becke, A.D. Density-Functional Thermochemistry. III. The Role of Exact Exchange. *J. Chem. Phys.* **1993**, *98*, 5648–5652. [[CrossRef](#)]
49. Da Chai, J.; Head-Gordon, M. Long-Range Corrected Hybrid Density Functionals with Damped Atom-Atom Dispersion Corrections. *Phys. Chem. Chem. Phys.* **2008**, *10*, 6615–6620. [[CrossRef](#)] [[PubMed](#)]
50. Szori, M.; Abou-Abdo, T.; Fittschen, C.; Csizmadia, I.G.; Viskolcz, B. Allylic Hydrogen Abstraction II. H-Abstraction from 1,4 Type Polyalkenes as a Model for Free Radical Trapping by Polyunsaturated Fatty Acids (PUFAs). *Phys. Chem. Chem. Phys.* **2007**, *9*, 1931–1940. [[CrossRef](#)] [[PubMed](#)]
51. Szori, M.; Fittschen, C.; Csizmadia, I.G.; Viskolcz, B. Allylic H-Abstraction Mechanism: The Potential Energy Surface of the Reaction of Propene with OH Radical. *J. Chem. Theory Comput.* **2006**, *2*, 1575–1586. [[CrossRef](#)]
52. Izsák, R.; Szori, M.; Knowles, P.J.; Viskolcz, B. High Accuracy Ab Initio Calculations on Reactions of OH with 1-Alkenes. The Case of Propene. *J. Chem. Theory Comput.* **2009**, *5*, 2313–2321. [[CrossRef](#)]
53. Curtiss, L.A.; Redfern, P.C.; Raghavachari, K.; Rassolov, V.; Pople, J.A. Gaussian-3 Theory Using Reduced Møller-Plesset Order. *J. Chem. Phys.* **1999**, *110*, 4703–4709. [[CrossRef](#)]
54. Janoschek, R.; Rossi, M.J. Thermochemical Properties of Free Radicals from G3MP2B3 Calculations. *Int. J. Chem. Kinet.* **2002**, *34*, 550–560. [[CrossRef](#)]
55. Frisch, M.; Trucks, G.W.; Schlegel, H.B.; Scuseria, G.E.; Robb, M.A.; Cheeseman, J.R.; Scalmani, G.; Barone, V.; Mennucci, B.; Fox, D.J. *Gaussian 09, Revision E.01*; Gaussian Inc.: Wallingford, CT, USA, 2013.
56. Legault, C.Y. *CYLVIEW, V1.0561*; Université de Sherbrooke: Sherbrooke, QC, Canada, 2009.

Disclaimer/Publisher's Note: The statements, opinions and data contained in all publications are solely those of the individual author(s) and contributor(s) and not of MDPI and/or the editor(s). MDPI and/or the editor(s) disclaim responsibility for any injury to people or property resulting from any ideas, methods, instructions or products referred to in the content.